

Discovery of Imidazo[1,2-a]pyrazines and Pyrazolo[1,5-c]pyrimidines as TARP #8 Selective AMPAR Negative Modulators

Brad M. Savall, Dongpei Wu, Devin Maun Swanson, Mark Seierstad, Nyantsz Wu, Jorge Vives Martinez, Beatriz Garcia Olmos, Brian Lord, Kevin J Coe, Tatiana Koudriakova, Timothy W Lovenberg, Nicholas I. Carruthers, Michael P. Maher, and Michael K. Ameriks

ACS Med. Chem. Lett., **Just Accepted Manuscript** • DOI: 10.1021/acsmchemlett.8b00599 • Publication Date (Web): 26 Dec 2018

Downloaded from <http://pubs.acs.org> on December 27, 2018

Just Accepted

“Just Accepted” manuscripts have been peer-reviewed and accepted for publication. They are posted online prior to technical editing, formatting for publication and author proofing. The American Chemical Society provides “Just Accepted” as a service to the research community to expedite the dissemination of scientific material as soon as possible after acceptance. “Just Accepted” manuscripts appear in full in PDF format accompanied by an HTML abstract. “Just Accepted” manuscripts have been fully peer reviewed, but should not be considered the official version of record. They are citable by the Digital Object Identifier (DOI®). “Just Accepted” is an optional service offered to authors. Therefore, the “Just Accepted” Web site may not include all articles that will be published in the journal. After a manuscript is technically edited and formatted, it will be removed from the “Just Accepted” Web site and published as an ASAP article. Note that technical editing may introduce minor changes to the manuscript text and/or graphics which could affect content, and all legal disclaimers and ethical guidelines that apply to the journal pertain. ACS cannot be held responsible for errors or consequences arising from the use of information contained in these “Just Accepted” manuscripts.



Discovery of Imidazo[1,2-*a*]pyrazines and Pyrazolo[1,5-*c*]pyrimidines as TARP γ -8 Selective AMPAR Negative Modulators

Brad M. Savall[‡], Dongpei Wu[†], Devin M. Swanson[†], Mark Seierstad[†], Nyantsz Wu[†], Jorge Vives Martinez[⊥], Beatriz García Olmos[⊥], Brian Lord[†], Kevin Coe[†], Tatiana Koudriakova[†], Timothy W. Lovenberg[†], Nicholas I. Carruthers[†], Michael P. Maher[†], and Michael K. Ameriks^{*†}

[†]Janssen Research & Development L.L.C., 3210 Merryfield Row, San Diego, CA 92121 United States

[‡]Sanford Burnham Prebys Medical Discovery Institute, 10901 N. Torrey Pines Rd., La Jolla, CA 92037 United States

[⊥]Eurofins-Villapharma Research S.L., Parque Tecnológico de Fuente Alamo, Carretera El Estrecho-Lobosilo, Km. 2,5, E-30320, Fuente Alamo (Murcia), Spain

KEYWORDS AMPA, α -amino-3-hydroxy-5-methyl-4-isoxazolepropionic acid, AMPA, TARP γ -8, transmembrane AMPA receptor regulatory protein, auxiliary subunit, glutamate, hippocampus, epilepsy, glutathione, autoradiography

ABSTRACT: This report discloses the discovery and characterization of imidazo[1,2-*a*]pyrazines and pyrazolo[1,5-*c*]pyrimidines as selective negative modulators of α -amino-3-hydroxy-5-methylisoxazole-4-propionate receptors (AMPA) associated with transmembrane AMPAR regulatory protein (TARP) γ -8. Imidazopyrazine **5** was initially identified as a promising γ -8 selective HTS hit, and subsequent SAR optimization yielded sub-nanomolar, brain penetrant leads. Replacement of the imidazopyrazine core with an isosteric pyrazolopyrimidine scaffold improved microsomal stability and efflux liabilities to provide **26**, JNJ-61432059. Following oral administration, **26** exhibited time- and dose-dependent AMPAR/ γ -8 receptor occupancy in mouse hippocampus, which resulted in robust seizure protection in corneal kindling and pentylenetetrazole (PTZ) anticonvulsant models.

Glutamate is the primary excitatory neurotransmitter in the central nervous system (CNS), where it functions as an agonist at several metabotropic (mGluR) and ionotropic (iGluR) receptors. The α -amino-3-hydroxy-5-methyl-4-isoxazole propionic acid (AMPA) subtype of ionotropic glutamate receptors mediates fast synaptic transmission within the CNS and plays a critical role in modulating synaptic plasticity.¹ AMPA receptors (AMPA) are assembled as tetramers of pore-forming subunits (GluA1-GluA4) together with a host of accessory proteins that work in concert to regulate receptor trafficking and pharmacology. Most, if not all, AMPARs are associated with transmembrane AMPAR regulatory proteins (TARPs), which are classified by sequence homology and function as Type I (γ -2, γ -3, γ -4, γ -8) or Type II (γ -5, γ -7).² Whereas GluA subunits are widely distributed as heteromeric complexes throughout the brain, several TARPs exhibit more discrete expression patterns. In particular, TARP γ -8 is highly enriched in the hippocampus as well as certain subregions of the forebrain, with minimal localization in the cerebellum or brainstem.³ Accordingly, in rodents, selective negative modulation of AMPARs associated with γ -8 has been shown to attenuate hyperexcitability in the hippocampus without direct effects on the midbrain or hind brain.⁴⁻⁶ Since excitatory neurotransmission plays a key role in seizure generation and propagation, selective AMPAR/TARP γ -8 negative modulators are expected to function as effective anticonvulsants with an improved therapeutic index relative to current standards of care, which affect synaptic transmission throughout the brain.⁷

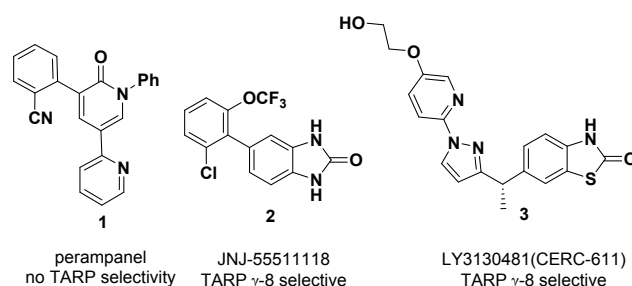


Figure 1. Representative AMPAR negative modulators

Several classes of AMPAR negative allosteric modulators have been disclosed previously (Figure 1). These include non-competitive AMPAR antagonists, such as perampanel (**1**), which bind at the interface between the ion-channel and the ligand binding domain.⁸ Although perampanel is an FDA-approved adjunctive treatment for uncontrolled partial-onset seizures, CNS-related side-effects such as dizziness, sedation, and falling have been reported at therapeutically relevant doses.⁹ Perampanel is not a TARP-selective antagonist, and inhibition of AMPARs associated with stargazin (γ -2), the primary TARP expressed in cerebellum, may contribute to the motor impairment observed in patients.¹⁰ Recently, several AMPAR negative modulators selective for γ -8 have been reported, including JNJ-55511118^{5,11} (**2**) and LY3130481/CERC-611¹² (**3**). These compounds appear to partially disrupt an important protein-protein interaction between the TARP and the pore-forming subunit of the ion-

channel.^{4-6,13} Herein, we describe the discovery, optimization, and *in vivo* characterization of a structurally distinct class of substituted imidazo[1,2-*a*]pyrazine and pyrazolo[1,5-*c*]pyrimidine-based selective AMPAR/ γ -8 negative modulators.

A high-throughput screening (HTS) campaign identified compounds that blocked glutamate-induced Ca²⁺ flux in HEK-293 cells expressing a fusion protein between γ -8 and the GluA1 α “flop” splice variant.⁵ Confirmed hits were counter-screened in heterologous cells co-transfected with GluA1 α and γ -2. From this effort, benzimidazole **4** and imidazo[1,2-*a*]pyrazine **5** emerged as preliminary leads due to their encouraging potency and selectivity for γ -8 (Figure 2). Whereas **4** moderately inhibited Ca²⁺ flux in cells expressing GluA1/ γ -2 (pIC₅₀ = 5.9), **5** was inactive towards γ -2 at the highest concentrations tested (100 μ M). Furthermore, whole cell electrophysiology confirmed that **5** inhibited time-dependent AMPA responses to glutamate in acutely dissociated rat hippocampal neurons, but not rat cerebellar Purkinje neurons (Supplementary Figure 1). Specifically, in hippocampal neurons, a saturating concentration of **5** (10 μ M) partially reduced peak currents (~50% inhibition) and completely blocked steady-state currents evoked by 10 mM L-glutamate, which is similar in magnitude to the effects observed with previously disclosed AMPAR/ γ -8 selective negative modulators.^{5,6}

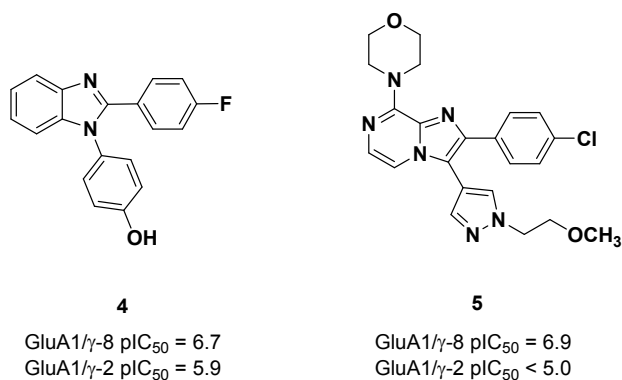


Figure 2. AMPAR/ γ -8 selective HTS hits

Comparison of the two HTS leads suggested merging structural elements through replacement of the substituted pyrazole in **5** with the phenol in **4** to generate hybrid analog **6** (Table 1). Gratifyingly, imidazopyrazine **6** was 10-fold more potent than **5** and maintained exquisite selectivity over γ -2. Incorporation of a *para*-fluorophenyl group in the 2-position (**7**) retained potency and improved lipophilic ligand efficiency relative to *para*-chlorophenyl **6**. Consequently, the *para*-fluorophenyl moiety was held constant at C-2 while scanning aromatic groups in the 3-position. The dramatic difference in potency between phenol **7** (pIC₅₀ = 7.9) and methoxyphenyl **8** (pIC₅₀ = 6.3) implicated the importance of a hydrogen-bond donor in the *para* position. Relative to the phenol, aniline **9** was less potent (pIC₅₀ = 7.2), and acylation of the amine (**10**) completely ablated activity. However, constraining the hydrogen bond donor within a ring dramatically improved potency, as both oxindole **11** and indazole **12** were sub-nanomolar compounds. In all cases, no inhibition of γ -2 was ever observed.

Table 1. Initial imidazo[1,2-*a*]pyrazine SAR

Cmpd	R	X	GluA1/ γ -8 pIC ₅₀ ^a	GluA1/ γ -2 pIC ₅₀ ^b	LLE
6		Cl	8.0 ± 0.3	< 5.0	3.7
7		F	7.9 ± 0.1	< 5.0	4.2
8		F	6.3 ± 0.4	< 5.0	2.1
9		F	7.2 ± 0.3	< 5.0	4.1
10		F	< 5.0 (n = 1)	< 5.0	<1.6
11		F	9.3 ± 0.1	< 5.0	6.4
12		F	9.2 ± 0.2	< 5.0	5.5

^apIC₅₀ measured in a FLIPR assay using HEK-293 cells expressing a human GluA1 α - γ -8 fusion construct; unless noted, all data are the result of at least three assays run in triplicate with the mean value and standard deviation reported.

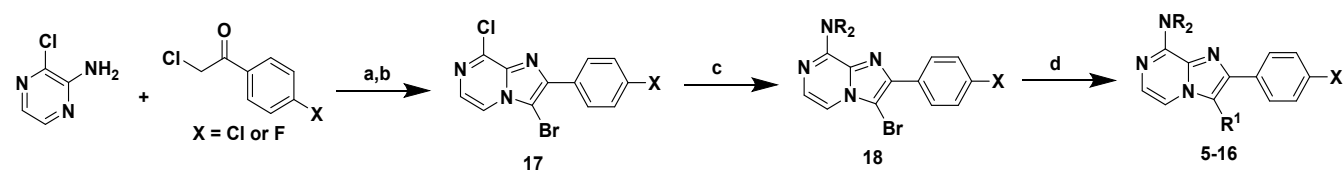
^bpIC₅₀ measured in a FLIPR assay using HEK-293 cells expressing human GluA1 α co-transfected with γ -2.

Although **11** and **12** displayed similar γ -8 potency, cross-reactivity with numerous CYP isozymes (i.e. 2C9 IC₅₀ = 500 nM) prevented further progression of indazole **12**. Consequently, the oxindole group was selected as a preferred arene at C-3 and held fixed during further SAR optimization around the C-8 position (Table 2). Several substituted cyclic amines maintained the promising γ -8 potency of the parent morpholine **11**, and 4-fluoropiperidine **14** was especially impressive in this regard (IC₅₀ = 100 pM). In addition, these morpholine replacements provided marginal improvements in both human and rat liver microsome stability, although often at the expense of increased Pgp-mediated efflux in a MDCK-MDR1 permeability assay. Subsequent *in vivo* profiling in rat revealed that brain penetration correlated well with *in vitro* efflux ratios, as the compounds with the lowest predicted efflux (**11** and **14**) also exhibited the highest unbound brain partition coefficients (K_{p,u} > 0.3). Unfortunately, all imidazopyrazines profiled *in vivo* suffered from low to moderate bioavailability and high clearance, sometimes greater than hepatic blood flow (i.e. **14**, Cl = 86 mL/min/kg).

Table 2. SAR and profile of 8-substituted imidazo[1,2-*a*]pyrazine derivatives


Cmpd	NR ₂	GluA1/γ-8 pIC ₅₀ ^a	GluA1/γ-2 pIC ₅₀ ^b	HLM/RLM stability ^c	MDCK-MDR1 ^d ratio/(A-B) x10 ⁻⁶ cm/s	rat PK parameters ^e			rat BBB ^f	
						Cl (mL/min/kg)	V _{ss} (L/kg)	%F	[brain]/[plasma] (ng/g) / (ng/mL)	K _{p,u} (brain)
11		9.3 ± 0.1	< 5.0	0.8 / 0.8	2.8 / 13	59 ± 12	3.2 ± 0.5	35 ± 15	205 / 105	0.33
13		9.4 ± 0.4	< 5.0	0.7 / 0.4	86 / 1.0	59 ± 11	2.4 ± 0.2	25 ± 3	39 / 270	0.03
14		10.0 ± 0.2	< 5.0	0.7 / 0.7	1.6 / 0.5	86 ± 13	5.9 ± 0.8	28 ± 9	231 / 137	0.56
15		9.3 ± 0.2	< 5.0	0.7 / 0.7	72 / 0.6	62 ± 11	2.2 ± 0.2	8 ± 2	11 / 214	0.01
16		9.4 ± 0.2	< 5.0	0.6 / 0.5	78 / 0.7	64 ± 4	2.5 ± 0.5	37 ± 7	25 / 130	0.06

^apIC₅₀ measured in FLIPR assay using HEK-293 cells expressing a human GluA1 α - γ -8 fusion construct; all data are the result of at least three assays run in triplicate with the mean value and standard deviation reported. ^bpIC₅₀ measured in a FLIPR assay using HEK-293 cells transiently expressing human GluA1 α co-transfected with γ 2 (n = 1, run in triplicate). ^cStability in human and rat liver microsomes at 1 μ M; data are reported as extraction ratios. ^dApparent permeability, reported as ratio of B to A direction/ A to B direction. ^eCompounds dosed as solutions in 20% HP- β -CD (cmpds **13,15,16**), 30% SBE-CD (cmpd **11**), or 50% PEG400/H₂O (cmpd **14**) at 1 mg/kg (i.v.) and 5 mg/kg (p.o.) in Sprague Dawley rats (n=3/group). ^fCompounds dosed as solutions in 20% HP- β -CD at 10 mg/kg (p.o.) Sprague Dawley rats (n=2/group). Details for all assay conditions are provided in the supplemental information.

Scheme 1. Synthesis of imidazo[1,2-*a*]pyrazines **5-16**^a

^aReagents and conditions: (a) Et₂NPh, CH₃CN or CH₃CH₂CN, reflux, 50-54%; (b) NBS, CH₂Cl₂, 69-85%; (c) R₂NH, Et₃N or iPrNEt₂, CH₃CN, 80 °C, 75-87%; (d) R¹B(OH)₂, Pd(PPh₃)₄, 1:1 dioxane/1M Na₂CO₃, μ wave, 110°C, 57-86%.

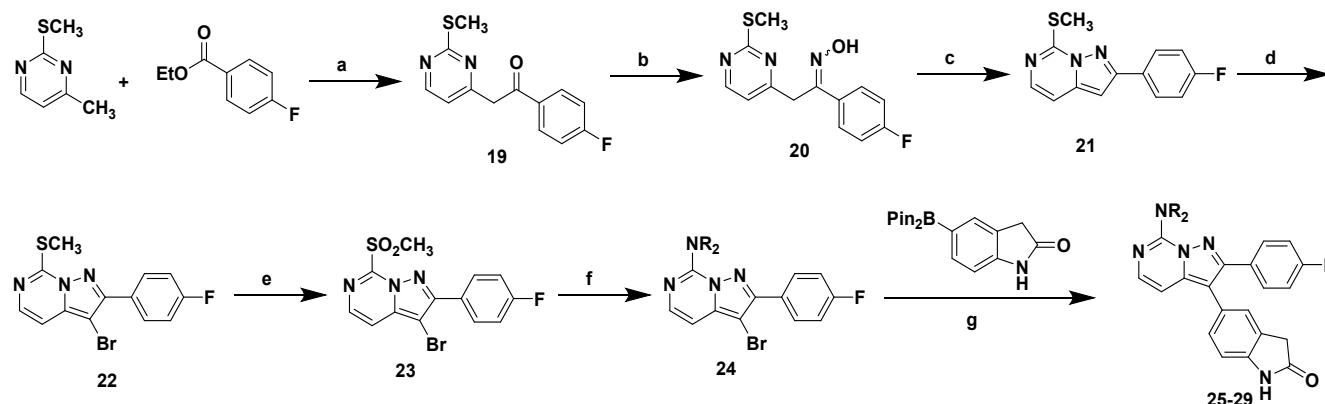
Imidazo[1,2-*a*]pyrazines **5-16** were prepared using the synthetic sequence shown in Scheme 1.¹⁴ Specifically, condensation of 2-amino-3-chloropyrazine with α -chloro-*para*-fluoro-acetophenone, followed by bromination, afforded a key dihalo imidazopyrazine intermediate **17**. Selective displacement of the 8-chloro group was achieved by heating with an amine to deliver **18**, which was then functionalized at the 3-position through Suzuki couplings.

To mitigate the poor PK properties of the imidazopyrazine series, several core replacements were investigated. Ultimately,

an isosteric pyrazolo[1,5-*c*]pyrimidine scaffold showed the most promise (Scheme 2). This 6,5-heterocycle was assembled through an initial condensation between 4-methyl-2-(methylthio)pyrimidine and *para*-fluorophenyl ethyl benzoate to give ketone **19**, followed by conversion to oxime **20** and an iron-mediated ring closure to form the core **21**.¹⁵ Bromination at the 3-position (**22**) preceded sulfide oxidation to provide an important sulfone intermediate (**23**). Functionalization at C-7 was accomplished using S_NAr displacements with a variety of

amines (**24**), and the C-3 oxindole was installed via a dppf-mediated Suzuki reaction to afford the final products **25-29**.

Scheme 2. Synthesis of pyrazolo[1,5-*c*]pyrimidines **25-29**^a



^aReagents and conditions: (a) LiHMDS, THF, rt \rightarrow 45 °C, 85%; (b) H₂NOH-HCl, 3M NaOH, MeOH, 65 °C, 50%; (c) Et₃N, TFAA, 0.3 eq FeCl₂, DME, 80 °C, 53%; (d) NBS, CH₃CN, rt, 82%; (e) mCPBA, NaHCO₃, CH₂Cl₂, 0 °C, 100%; (f) R₂NH, DMA, 100 °C, 40-67%; (g) cat Pd(dtbpf)Cl₂, NaHCO₃, dioxane/water, 110 °C, 17-76%.

Table 3. SAR and profile of pyrazolo[1,5-*c*]pyrimidines **25-29**

Cmpd	NR ₂	GluA1/γ-8 pIC ₅₀ ^{a,b}	HLM/RLM stability ^c	MDCK-MDR1 ^d efflux ratio/(A-B)
25		9.3 ± 0.3	0.8 / 0.6	1.9 / 8.5
26		9.7 ± 0.5	0.6 / 0.5	13 / 3.3
27		8.3 ± 1.2	0.6 / 0.6	ND ^e / 1.2
28		8.3 ± 0.7	0.7 / 0.6	135 / 0.3
29		9.6 ± 0.3	0.6 / 0.5	34 / 2.1

^apIC₅₀ measured in a FLIPR assay using HEK-293 cells expressing a human GluA1 α -γ-8 fusion construct; all data are the result of at least three assays run in triplicate with the mean value and standard deviation reported. ^bAll compounds tested had pIC₅₀ < 5 at GluA1/γ-2. ^cStability in human and rat liver microsomes at 1 μM; data are reported as extraction ratios. ^dApparent permeability (×10⁻⁶ cm/s) reported as ratio of B to A direction/ A to B direction. ^eNot determined due to poor compound recovery in the B to A direction. Details for all assay conditions are provided in the supplemental information.

SAR and select *in vitro* data for pyrazolopyrimidines **25-29** are shown in Table 3. Although switching from the imidazopyrazine to pyrazolopyrimidine core resulted in a loss of potency for several compounds (see Table 2; compare **14/27**, as well as **15/28**), other homologs retained activity (compare **11/25**, **13/26**, and **16/29**). Furthermore, a majority of the pyrazolopyrimidine analogs displayed lower efflux ratios, as well as improved stability in human liver microsomes, relative to their imidazopyrazine matched pairs. Hydroxypiperidine **26** (JNJ-61432059) appeared especially promising, and further characterization confirmed that this compound was highly selective for AMPAR/γ-8. When tested at 10 μM, **26** did not inhibit glutamate-induced calcium-flux in heterologous cells that co-expressed AMPARs with any TARP other than γ-8 (Supplementary Table 1). In addition, no cross-reactivity was noted when **26** was screened against a panel of 52 receptors, ion channels, and transporters using radioligand displacement assays (<50% inh @ 1 μM; Eurofins/Cerep, Poitiers, France). Furthermore, at concentrations as high as 10 μM, **26** did not displace [³H]dofetilide in a hERG binding assay, although inhibition of CYPs 2C8 and 2C9 were noted at lower concentrations (IC₅₀s = 3.0 and 1.9 μM, respectively).

Due to its encouraging *in vitro* profile, **26** was further evaluated *in vivo*. After oral dosing at 10 mg/kg in rats, **26** distributed into the brain (K_{p,u} = 0.4) despite low plasma exposures (C_{max} = 26 ng/mL) and high clearance (Cl = 57 mL/min/kg). The high *in vivo* clearance was unexpected based on the extraction ratio estimated from rat liver microsomes. A subsequent cross-species metabolite ID study revealed that the higher than anticipated clearance was likely due to a rat-specific UGT-mediated glucuronidation. Specifically, when **26** was incubated with hepatocytes for 4h at 37 °C, the O-glucuronide was detected as the major metabolite in rat, but only as a minor metabolite in human, mouse, dog, and monkey hepatocytes.

This species-specific metabolism was further supported by mouse PK studies, in which **26** displayed improved clearance (40 mL/min/kg) and ~80-fold higher plasma exposures (C_{max} = 2037 ng/mL) compared to an equivalent dose in rat. Furthermore, when administered orally at 10 mg/kg, **26** showed

high target engagement in mouse hippocampus, as measured by *ex vivo* autoradiography⁵, with maximal receptor occupancy exceeding 90% at one hour (Figure 3, top panel). The plasma and brain exposures at T_{\max} were highly linear over a wide dose range, and the receptor occupancy was well-described by a Hill function with $ED_{50} = 2.9 \pm 0.7$ mg/kg (Figure 3, bottom panel). Fitting the occupancy as a function of exposure, this corresponds to an $EC_{50} = 77 \pm 7$ ng/g in brain and 362 ± 59 ng/mL in plasma.

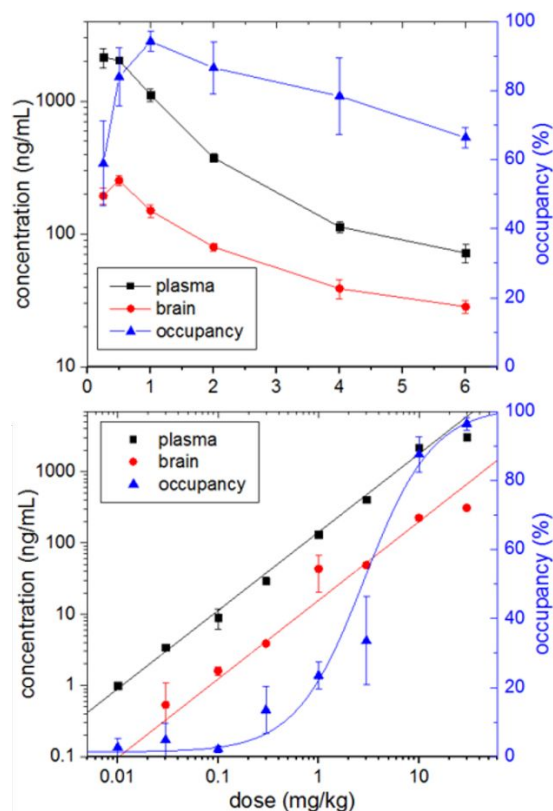


Figure 3. Exposures and GluA/ γ -8 receptor occupancy for compound **26** in mouse. (Top panel) Time dependency following single p.o. dose (10 mg/kg, $n = 3/\text{time point} + \text{SEM}$). (Bottom panel) Dose dependency following p.o. administration ($n=3/\text{dose} \pm \text{SEM}$). Receptor occupancy was measured by *ex vivo* ARG as described previously using [³H] JNJ-56022486 as the radiotracer.⁵

Based on the robust target engagement observed *in vivo*, **26** was evaluated in several mouse seizure models. Protection in the corneal kindling model was nearly complete at saturating doses, with an $ED_{50} = 1.3 \pm 0.1$ mg/kg (Figure 4, left panel, black curve). Seizure protection did not attenuate after 5 days of continued oral dosing at 5 mg/kg/day, indicating that there was no tolerance to drug treatment (Figure 4, middle panel, red line).¹⁶ To assess potential compound-related effects on motor function, all animals were subjected to the rotarod test immediately prior to seizure challenge. At all doses tested, no ataxia was observed (Figure 4, left and middle panels, blue lines). In the i.v. pentylenetetrazole (PTZ) test, the threshold amounts of PTZ required to generate twitch and clonus were increased after a single 5 mg/kg oral dose of **26** (Figure 4, right panel). As with the corneal kindling model, anticonvulsant efficacy was maintained after chronic administration as well (5 mg/kg/day).

In summary, we have described the discovery, optimization, and *in vivo* characterization of imidazo[1,2-*a*]pyrazines and pyrazolo[1,5-*c*]pyrimidines as AMPAR modulators selective for TARP γ -8. Starting from HTS hits **4** and **5**, a focused medicinal chemistry effort provided a series of potent and selective imidazopyrazine leads. Although brain penetrant compounds from this chemotype could be identified, high *in vivo* clearance prevented further development. Replacement of the imidazopyrazine scaffold with an isosteric pyrazolopyrimidine core improved microsomal stability and efflux liabilities, ultimately delivering compound **26** (JNJ-61432059). Following oral administration, **26** exhibited time- and dose-dependent receptor occupancy in mouse hippocampus. In addition, after acute and chronic dosing, **26** provided robust protection in rodent seizure models without adversely affecting motor function. This preclinical profile provides further support for the development of selective AMPAR/ γ -8 negative modulators as novel, differentiated antiepileptics.

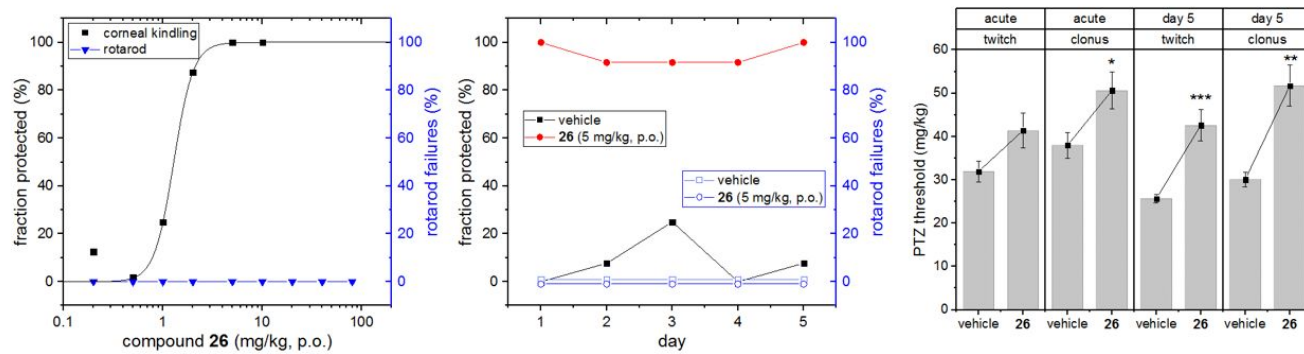


Figure 4. Anticonvulsant models. (Left panel) Protection as a function of dose in the mouse corneal kindling model for compound **26**. $N = 8-11$ mice/cohort. Animals were tested at $t = 1$ h following oral dosing, and data show fraction of animals with Racine scores of 3 or lower

(black curve). Rotarod failure data (blue curve) represent the fraction of animals in each cohort that failed a rotarod test immediately prior to seizure challenge. (Middle panel) Fraction of animals protected in the corneal kindling model (red line) tested at $t = 1$ h following once-daily oral dosing of compound **26** (5 mg/kg/day; $N = 12-14$ animals per cohort). (Right panel) Intravenous PTZ test at $t = 2$ h following a single (acute) or 5 days of once-daily (day 5) oral dosing with 5 mg/kg of compound **26** ($N = 9-11$ per cohort).

ASSOCIATED CONTENT

Supporting Information. Experimental procedures, characterization, and assay conditions. This material is available free of charge via the Internet at <http://pubs.acs.org>

AUTHOR INFORMATION

Corresponding Author

* mameriks@its.jnj.com

Author Contributions

All authors have given approval to the final version of the manuscript.

Notes

The authors declare no competing financial interest.

ACKNOWLEDGMENT

The authors acknowledge the contributions of the following individuals associated with Janssen Research and Development for their contributions to the work described here: Ning Qin cloned several of the GluA and TARP genes and generated the expression constructs. Hong Yu and Jose Matta conducted electrophysiology experiments in neurons. Raymond Rynberg developed formulations for several *in vivo* experiments. Leslie Nguyen, Minerva Batugo, Xiaohui Jiang, and Brian Scott performed the bioanalytical studies. H. Steve White and Cameron Metcalf at NeuroAdjuvants, Inc. performed the anticonvulsant studies.

ABBREVIATIONS

AMPA, α -amino-3-hydroxy-5-methyl-4-isoxazolepropionic acid; TARP, transmembrane AMPA receptor regulatory protein; CNS, central nervous system; FDA, Food and Drug Administration; LLE, ligand-lipophilicity efficiency; ADME, absorption, distribution, metabolism, excretion; DMPK, drug metabolism and pharmacokinetics; SAR, structure-activity relationship; CYP, cytochrome P450; FLIPR, fluorescence imaging plate reader; p.o., per os; i.v., intravenous; PK, pharmacokinetics; CL, clearance; V_{ss} , volume of distribution at steady state; $t_{1/2}$, half-life; C_{max} , maximum concentration; F, bioavailability; RLM, rat liver microsome; HLM, human liver microsome; $K_{p,u}$, partition coefficient for unbound compound concentration in tissue of interest relative to unbound concentration in plasma; BBB, blood-brain-barrier; MDR1, multi-drug resistance gene; MDCK-MDR1, Madin Darby canine kidney cell line transfected with MDR1; RO, receptor occupancy; HP- β -CD, (2-hydroxypropyl)- β -cyclodextrin; SBE-CD, sulfobutylether- β -cyclodextrin; PEG, polyethylene glycol; SEM, standard error of the mean; PTZ, pentylentetrazole

REFERENCES

- (1) Huganir, R.L.; Nicoll, R.A. AMPARs and synaptic plasticity: the last 25 years. *Neuron*, **2013**, *80*, 704-717.
- (2) Jackson, A.C.; Nicoll, R.A. The expanding social network of ionotropic glutamate receptors: TARPs and other transmembrane auxiliary subunits. *Neuron*, **2011**, *70*, 178-199.

(3) Tomita, S.; Chen, L.; Kawasaki, Y.; Petralia, R.S.; Wenthold, R.J.; Nicoll, R.A.; Brecht, D.S. Functional studies and distribution define a family of transmembrane AMPA receptor regulatory proteins. *J. Cell Biol.*, **2003**, *161*(4), 805-815.

(4) Maher, M.P.; Matta, J.A.; Gu, S.; Seierstad, M.; Brecht, D.S. Getting a handle on neuropharmacology by targeting receptor-associated proteins. *Neuron*, **2017**, *96*, 989-998.

(5) Maher, M.P.; Wu, N.; Ravula, S.; Ameriks, M.K.; Savall, B.M.; Liu, C.; Lord, B.; Wyatt, R.M.; Matta, J.A.; Dugovic, C.; et al. Discovery and characterization of AMPA receptor modulators selective for TARP- γ 8. *J. Pharmacol. Exp. Ther.*, **2016**, *357*, 394-414.

(6) Kato, A.S.; Burris, K.D.; Gardinier, K.M.; Gernert, D.L.; Porter, W.J.; Reel, J.; Ding, C.; Tu, Y.; Schober, D.A.; Lee, M.R., et al. Forebrain-selective AMPA-receptor antagonism guided by TARP γ -8 as an antiepileptic mechanism. *Nat. Med.*, **2016**, *22*, 1496-1501.

(7) Rogawski, M.A. Revisiting AMPA receptors as an antiepileptic drug target. *Epilepsy Curr.*, **2011**, *11*, 56-63.

(8) Yelshanskaya, M.V.; Singh, A.K.; Sampson, J.M.; Narangoda, C.; Kurnikova, M.; Sobolevsky, A.I. Structural bases of non-competitive inhibition of AMPA-subtype ionotropic glutamate receptors by antiepileptic drugs. *Neuron*, **2016**, *91*, 1305-1315.

(9) Greenwood, J.; Valdes, J. Perampanel (Fycompa) a review of clinical efficacy and safety in epilepsy. *P T*, **2016**, *41*(11), 683-688.

(10) Chen, L.; Chetkovich, D.M.; Petralia, R.S.; Sweeney, N.T.; Kawasaki, Y.; Wenthold, R.J.; Brecht, D.S.; Nicoll, R.A. Stargazin regulates synaptic targeting of AMPA receptors by two distinct mechanisms. *Nature*, **2000**, *408*, 936-943.

(11) Ravula, S.; Savall, B.M.; Wu, N.; Lord, B.; Coe, K.; Wang, K.; Seierstad, M.; Swanson, D.M.; Ziff, J.; Nguyen, M.; Leung, P.; Rynberg, R.; La, D.; Pippel, D.J.; Koudriakova, T.; Lovenberg, T.W.; Carruthers, N.I.; Maher, M.P.; Ameriks, M.K. *ACS MedChem Lett*, **2018**, *9*(8), 821-826.

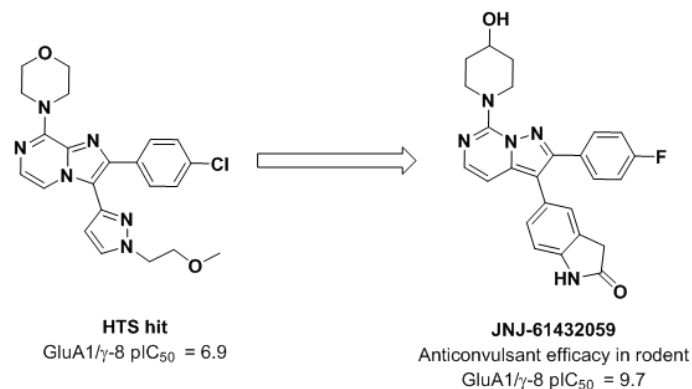
(12) Gardinier, K.M.; Gernert, D.L.; Porter, W.J.; Reel, J.K.; Ornstein, P.L.; Spinazze, P.; Stevens, F.C.; Hahn, P.; Hollinshead, S.P.; Mayhugh, D., et al. Discovery of the first α -amino-3-hydroxy-5-methyl-4-isoxazolepropionic acid (AMPA) receptor antagonist dependent upon transmembrane AMPA receptor regulatory protein (TARP) γ -8. *J. Med. Chem.*, **2016**, *59*, 4753-4768.

(13) Lee, M.R.; Gardinier, K.M.; Gernert, D.L.; Schober, D.A.; Wright, R.A.; Wang, H.; Qian, Y.; Witkin, J.M.; Nisenbaum, E.S.; Kato, A.S. Structural determinants of the γ -8 TARP dependent AMPA receptor antagonist. *ACS Chem. Neurosci.*, **2017**, *8*(12), 2631-2647.

(14) Belanger, D.B.; Curran, P.J.; Hruza, A.; Voigt, J.; Meng, Z.; Mandal, A.K.; Siddiqui, M.A.; Basso, A.D.; Gray, K. Discovery of imidazo[1,2-a]pyrazine-based aurora kinase inhibitors. *Bioorg. Med. Chem. Lett.*, **2010**, *20*(17), 5170-5174.

(15) Gudmundsson, K.S.; Johns, B.A.; Weatherhead, J. Pyrazolopyrimidines and pyrazolotriazines with potent activity against herpes viruses. *Bioorg. Med. Chem. Lett.* **2009**, *19*(19), 5689-5692.

(16) Loscher, W.; Schmidt, D.; Experimental and clinical evidence for loss of efficacy (tolerance) during prolonged treatment with antiepileptic drugs. *Epilepsia*, **2006**, *47*(8), 1253-1284.



For Table of Contents Only